D. Nafpaktitis[1],
F. Paterakis[1,2],
M. Darwish[2],
G. Hloupis[1,*]

Regular paper

The Equal Areas Pulse Width Modulation (EAPWM) Method: an alternative approach to programmed PWM schemes

This paper investigates a direct approach to programmed PWM modelling directed to simplification of implementation. Analytical equations of Equal Areas Pulse Width Modulation (EAPWM) method are presented along with harmonic analysis results for odd number of pulses in half period of a 3-level single phase VSI. Simulation and practical work is being presented also. Estimation of the marginal modulation index has been carried out, inside the linear region of operation. The proposed method provides a rigid framework since it lies on a well-defined mathematical formulation without the need of large computational effort.

1. Introduction

In recent years several PWM techniques have been proposed for controlling the AC output of power electronic converters. The primary objective for all PWM schemes is to calculate the converter switching-on times in order to create the desired target output voltage [1]. The available schemes can be broadly classified as carrier-modulated PWM and programmed PWM schemes. Carrier modulated PWM schemes can be described by three fundamental types: modulation using naturally sampled sine wave-modulating wave intersections, regular sampling defined by sine wave-modulating wave intersections [2] and direct modulation [3]. The most common carrier based strategies are Sinusoidal PWM, Third Harmonic Injected PWM, Discontinuous or Dead Band PWM [4]. The actual PWM process in carrier modulated PWM methods is usually a simple comparison between a reference waveform and a saw tooth or a triangular carrier waveform. The ease of implementation on digital and analogue structures of these methods have made them widely accepted [5]. On the other hand the attenuation of wanted fundamental component of the output waveform, the increased switching frequencies and the generation of high frequency harmonic components previously not present, are their main drawbacks [6]. Sophisticated techniques such as PWM harmonic elimination [7], [8], [9], Optimised Space Vector PWM or Optimal Switching Pattern PWM [10] have been developed to overcome these drawbacks. Many PWM techniques have been proposed for the rising multilevel inverters including multicarrier PWM [11], or harmonic elimination with programmed PWM methods [12] or even based on genetic algorithms [13]. The main disadvantage of these programmed PWM techniques is that for their practical implementation complicated algorithms for transcendental equations need large computational power [14]. Each method

* Corresponding author: G. Hloupis, Technological Educational Institute of Athens, Dept. of Electronic Engineering, Egaleo, 12210, Athens, Greece, E-mail: hloupis@teiath.gr
[1] Technological Educational Institute of Athens, Dept. of Electronic Engineering, Egaleo, 12210, Greece
[2] Brunel University, School of Engineering & Design, Uxbribge, UB88PH, UK

has different characteristics, advantages and disadvantages regarding the ease of implementation, harmonic spectra and maximum modulation index or switching losses.

Towards to the direction of simplifying the implementation of a PWM based system, this paper presents the direct approach of programmed PWM modelling. The theory of equal areas that this paper is following has been presented in [3], [15] and [16]. The method has been analyzed and generalized for accurate production of the pulse-train with odd number of pulses. Simulation results are derived using MATLAB. The spectrum of the output is following the regular sampling discontinuous PWM pattern [2]. The total harmonic distortion is calculated using the equations derived for marginal values of the amplitude modulation ratio (m_a) inside the linear region of operation. Practical work has been carried out verifying the simulation results. The rest of the paper is divided in five parts. In the first part, a review of the first approach with linear segments of Equal Areas PWM is given. In the second part, the accurate and analytical method for the Equal Areas PWM (EAPWM) pulse-train generation is analyzed. In the third part, the harmonic analysis of the output using the FFT is carried out. In the fourth part the calculation for the marginal amplitude modulation ratio is presented followed by the calculation of the Total Harmonic Distortion THDv. In the last part simulation and experimental results are given.

2. Review of the equal areas theory using rectilinear segments

Nafpaktitis et al. [15], present and recapitulate the mathematical frame for the production of well-defined PWM pulses using equations that describe with satisfactory accuracy, not only the time that a palm appears, but its duration, as well. EAPWM method can be briefly described as follows: A sinusoidal voltage signal can be approximated using rectilinear segments which define intervals with duration d as depicted in Fig.1.
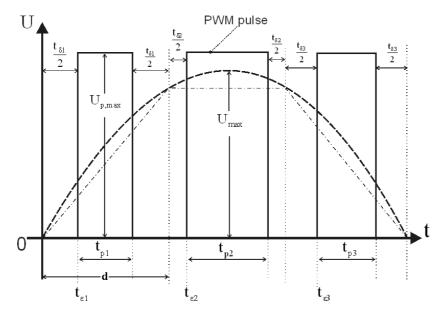

Figure 1. Approximation of sinusoidal voltage signal (dashed curve) by rectilinear segments (dot-dashed curve)

For each interval there is a corresponding pulse with amplitude U_{pmax}, active time t_P and inactive time t_δ. The active time t_P can be computed applying the condition of equal areas [15]. Each pulse is centered in its corresponding interval. In order to successfully

approximate sinusoidal signal using PWM, two crucial parameters are needed to be formulated: the pulse active time t_{pJ} at J interval and its corresponding firing time $t_{\varepsilon J}$. Both parameters were calculated as below:

$$t_{pJ} = \frac{d}{2} \cdot \frac{U_{max}}{U_{p\,max}} \left\{ \sin\left[(J-1)\omega \cdot d \right] + \sin(J \cdot \omega \cdot d) \right\}$$

(1)

$$t_{\varepsilon J} = (J-1)d + \frac{1}{2}(d - t_{pJ})$$

(2)

3. Generation of the optimized and accurate EAPWM pulse

An example for producing accurate EAPWM pulses is presented. In EAPWM only odd pulse numbers per half cycle will be studied. The reason for this is that since the maximum necessity for amplitude is needed at the middle of the sinus wave ($\pi/2$ and $3\pi/2$) then the centre pulse must be present in the PWM pulse train to produce the needed amplitude. Using Fig.2 and assuming that the half sinusoidal signal can be split in five equal intervals (with duration d), pulse's active time t_P (i.e. t_{p2} for the 2nd interval) can be found, beginning with the assumption that the area of the pulse (defined by ABCD points) must be equal with the area defined by EFGH points. Thus, using the integrals of the areas:

$$E_{ABCD} = E_{EFGH}$$

(3)

Eq.3 can be expressed as follows:

$$\omega t_{p2} U_{p\,max} = \int_{\omega d}^{2\omega d} U_{max} \sin(\omega t) d\omega t$$

(4)

Solving Eq.4 leads to

$$t_{p2} = \frac{U_{max}}{\omega \cdot U_{p\,max}} (\cos \omega d - \cos 2\omega d)$$

(5)

In generalized form, the pulse active time t_P in j interval will be:

$$t_{pJ} = \frac{U_{max}}{\omega \cdot U_{P\,max}} \left\{ \cos\left[(J-1)\omega d \right] - \cos(J\omega d) \right\}$$

(6)

Where *J* expresses the number of intervals (or equivalently the number of pulses A$_P$) that corresponds to a half period T/2 time. So, A$_P$ and d are related as follows:

$$A_p = \frac{0.5T}{d}$$

(7)

The switching frequency over a complete fundamental cycle is then calculated as:

$$f_s = \frac{1}{d} = \frac{2A_p}{T}$$

(8)

Yet, the phase leg switching frequency in discontinuous PWM schemes is modulated only for the 50% of the fundamental cycle (here can be expressed as f$_p$=Ap/T since only one phase leg is being modulated). The frequency modulation ratio is defined as m$_f$=f$_s$/f$_1$

and amplitude modulation ratio is defined as $m_a = U_{max}/U_{Pmax}$. For odd A_P there is a central pulse at positions T/4, 3T/4, 5T/4, 7T/4 etc where at sides exist $(A_P-1)/2$ symmetrical pulses. Using Eq.6 and Eq.2 we can calculate t_{Pj} active times and $t_{\varepsilon J}$ firing times respectively.
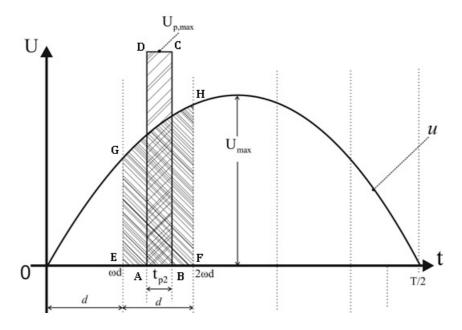

Figure 2.Generation of an accurate EAPWM pulse.

Recalling the generalized Fourier equations

$$u(t) = \{a_0/2 + a_1\cos\omega t + a_2\cos\omega t + a_3\cos\omega t + ... + b_1\cos\omega t + b_2\cos\omega t + b_3\cos\omega t + ...\} \quad (9)$$

$$a_n = \frac{1}{\pi}\int_0^{2\pi} u(t)\cos(n\omega t)d\omega t \quad (10)$$

$$b_n = \frac{1}{\pi}\int_0^{2\pi} u(t)\sin(n\omega t)d\omega t \quad (11)$$

The term $\alpha_0/2 = 0$ for *ac* signals. The coefficients α_n are also zero since the function u(t) is odd and the following equation holds

$$u(-t) = -u(t) \Rightarrow a_n = 0 \quad (12)$$

At the same time, the b_n coefficients are zero due to half wave symmetry

$$u(t) = -u(t + \frac{1}{2}T) \quad (13)$$

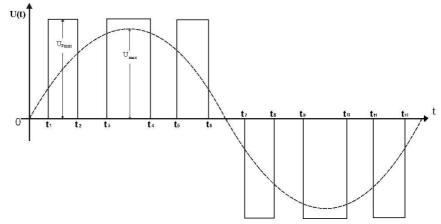the b_n coefficients are also zero for *n* even:

$$n : even \Rightarrow b_n = 0 \quad (14)$$

Figure 3.Time assignment at the beginning and at the end of each pulse.

Assigning the times t_1, t_2, t_3, t_4 ..... t_n at the beginning and the end of each pulse (as presented in Fig.3), the following equation for b_n coefficients is derived:

$$b_n = -\frac{4U_{p\max}}{n\pi}\left(-\cos(n\omega t_1)+\cos(n\omega t_2)-\cos(n\omega t_3)+.....-\cos(n\omega t_{A_p})\right) \tag{15}$$

where A_p defines the number of pulses. Eq.15 can be rearranged as below:

$$b_n = -\frac{4U_{p\max}}{n\pi}\sum_{k=1}^{k=A_p}(-1)^k\cos(n\omega t_k) \tag{16}$$

For the pulses' function u(t) it holds that:

$$u(t)=\left\{b_1\sin(\omega t)+b_3\sin(\omega t)+b_5\sin(\omega t)+.....+b_n\sin(\omega t)+.....\right\} \tag{17}$$

With *n* odd integer, it holds:

$$u(t)=\sum_{n=1,3,5,..}^{\infty}b_n\sin(n\omega t) \tag{18}$$

Or equivalently:

$$u(t)=\sum_{n=1,3,5,...}^{\infty}\left[-\frac{4U_{p\max}}{n\pi}\sum_{k=1}^{k=A_p}(-1)^k\cos(n\omega t_k)\right]\sin(n\omega t) \tag{19}$$

The firing and closing time t_k of the *J* pulse in respect to duration t_{pJ} and $t_{\varepsilon J}$

$$J=\frac{1+2k+(-1)^{k+1}}{4} \tag{20}$$

$$t_k=t_{\varepsilon J}+[\frac{1+(-1)^k}{2}]t_{pJ} \tag{21}$$

4. Evaluation of the Marginal m_a and Harmonic Analysis of the Voltage output.

The decrease of $U_{p,max}$ value, implies a corresponding increase at the duration of the pulse. The m_a cannot set higher than one because overlaps between the pulses will occur (first overlap is going to happen on the centred-middle pulse). The necessity here is to

decrease the $U_{p,max}$ in such a level where the corresponding duration of the pulse, t_p, will be less or equal to space ωd. Then, as shown in Fig.4, the $U_{p,max}$ will exist between U_{max} and $\overline{FE}$. The minimum $U_{p,max}$ ($U_{p,max-min}$, U_{pmm} hereafter) can be calculated using the equality that, the area ABCD must be equal with the hatched area ABEGF. This equality can be expressed as:
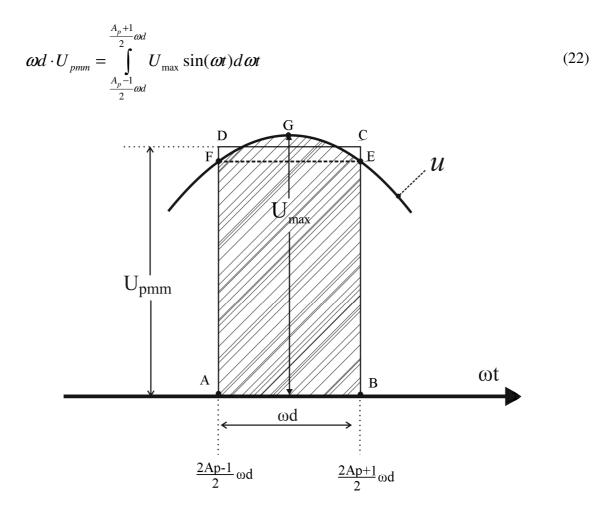
$$\omega d \cdot U_{pmm} = \int_{\frac{A_p-1}{2}\omega d}^{\frac{A_p+1}{2}\omega d} U_{max} \sin(\omega t) d\omega t \tag{22}$$

Figure 4. Calculation of U_{pmm}

Solving Eq.22 in relation to U_{pmm} becomes

$$U_{pmm} = U_{max} \frac{2A_p}{\pi} \sin\left(\frac{\pi}{2A_p}\right) \tag{23}$$

But since:

$$\lim_{A_p \to \infty} \left(\frac{2A_p}{\pi} \sin\left(\frac{\pi}{2A_p}\right)\right) = 1 \tag{24}$$

It holds that:

$$\lim_{A_p \to \infty} U_{pmm} = U_{max} \tag{25}$$

179

From Eq.25 one can deduce that for high switching frequency of pulse-train (high A_p values) the U_{pmm} coincides with U_{max}. Table 1 presents some indicative values of the optimum-marginal modulation index ratio (U_{max}/U_{pmm}) in relation with A_p that correspond to minimum THDv.

Table 1. Representative values of $m_a = U_{max}/U_{pmm}$ ratio in relation with A_p for minimum THDv

A_p	mf=fs/f1	ma=U_{max} / U_{pmm}
3	6	0.95493
5	10	0.98363
7	14	0.99163
…	…	…
15	30	0.99817
…	…	…
25	50	0.99934

5. Calculation of Total Harmonic Distortion

The Total Harmonic Distortion of Voltage is expressed (per cent) by the following expression:

$$THDv = 100\sqrt{\left(\frac{U_{rms}}{U_{1,rms}}\right)^2 - 1} \tag{26}$$

In order to calculate the THDv one must calculate the rms value of pulse-train, U_{rms} as well as the rms value of 1st harmonic of pulse-train, $U_{1,rms}$. For U_{rms} with $A_p=3$:

$$U_{rms} = U_{dc}\sqrt{\frac{2}{T}\left(2t_{p_1} + t_{p_2}\right)} \tag{27}$$

For $A_p=5$,

$$U_{rms} = U_{dc}\sqrt{\frac{2}{T}\left(2t_{p_1} + 2t_{p_2} + t_{p_3}\right)} \tag{28}$$

Eq.23 & Eq.24 concludes to a general expression for U_{rms}

$$U_{rms} = U_{dc}\sqrt{\frac{2}{T}\left(2t_{p_1} + 2t_{p_2} + ... + 2t_{p_{n-1}} + t_{p_n}\right)} \tag{29}$$

with $\quad n = \dfrac{1+A_p}{2}$

Substituting in Eq.29 , terms from Eq.6 and solve, many coefficients will be equal to zero. This will transform Eq.25 to a new expression:

$$U_{rms} = \sqrt{\frac{2 \cdot U_{grid} \cdot U_{dc}}{\pi} \left\{ 1 - 0.5 \cos\left[\left(\frac{A_p - 1}{2}\right)\frac{\pi}{A_p}\right] - 0.5\cos\left[\left(\frac{A_p + 1}{2}\right)\frac{\pi}{A_p}\right] \right\}} \tag{30}$$

It is easy to prove that the result between brackets equals 1. Thus,

$$U_{rms} = C \cdot \sqrt{U_{dc}}$$
$$\text{with} \quad C = \sqrt{\frac{2U_{grid}}{\pi}} \tag{31}$$

Eq.31 dictates that the voltage U_{rms} is independent by the number of pulses A_p and with constant U_{grid}, U_{rms} is affected only by U_{dc}.

The *rms* value of 1st harmonic, $U_{1,rms}$ can be calculated using Eq.15 as $U_{1,rms} = \dfrac{b_1}{\sqrt{2}}$ or

$$U_{1,rms} = 0.9 U_{dc}(\cos \omega t_1 + \cos \omega t_2 + ... + \cos \omega t_{A_p}) \tag{32}$$

Or alternatively

$$U_{1,rms} = -0.9 U_{dc} \sum_{k=1}^{k=A_p} (-1)^k \cos \omega t_k \tag{33}$$

The *k* coefficients and the times t_k derived from Eq.20 and Eq.21.

The minimum THDv corresponds to the best possible EAPWM pulse-train. This is achieved by increasing the frequency of pulse-train (high A_p values) or margining-"optimising" the value of the modulation index ratio $m_a = U_{max} / U_{pmm}$ using Eq.23.

Considering the values of U_{pmm} shown on Table 1 and using Eq.6 and Eq.23, the maximum active time for a pulse at interval *J* for U_{pmm}, can be calculated as below:

$$t_{pJ\max} = \frac{T}{4A_p} \frac{\left\{ \cos\left[(J-1)\frac{\pi}{A_p}\right] - \cos\left(J\frac{\pi}{A_p}\right) \right\}}{\sin \frac{\pi}{2A_p}} \tag{34}$$

Solving Eq.33 one can find that the limit of $U_{1,rms}$ for high values of A_p, is the rms value of sinusoidal voltage *u* (Eq.1) which is $U_{max}/\sqrt{2}$. Thus,

$$\lim_{A_p \to \infty} U_{1,rms} = \frac{U_{max}}{\sqrt{2}} \tag{35}$$

Substituting Eq.35 and Eq.31 to Eq.26 the minimum value of THDv holds as:

$$THDv_{\min} = 100 \sqrt{\frac{4 \cdot U_{p\max}}{\pi \cdot U_{max}} - 1} \tag{36}$$

From Eq.36 one can presume that for constant U_{max}, $THDv_{\min}$ is affected only by $U_{p,max}$ thus the ratio $m_a = U_{max} / U_{pmax}$.

In Fig.5 a range of THDv series vs. A_p is plotted, using the marginal modulation index ratio $m_a = U_{max} / U_{pmm}$. The number of pulse A_p indicates also the switching frequency as described in Eq.8. In Fig.5a, THDv is calculated using Eq.26. For $A_p > 11$ all the THDv values coincide to corresponding minimum values, $THDv_{\min}$. The U_{pmm} for $3 \geq A_p \geq 11$ is

lower even than U_{max}. For $A_p \geq 12$, THDv=THDv$_{min}$ which is 52.27% as calculated from Eq.36.

Since Eq.26 is applied to a full bridge inverter, it can be assumed that by proper control [18] the negative and positive semi-periods of the voltage output are symmetrical meaning no DC or even harmonics are present, the total harmonic distortion can be reduced to
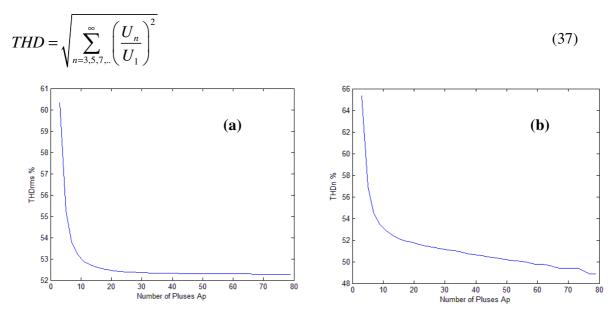
$$THD = \sqrt{\sum_{n=3,5,7,..}^{\infty} \left(\frac{U_n}{U_1}\right)^2} \tag{37}$$

Figure 5. THDv series vs. number of pulses (A_p) using marginal m_a, calculated by Eq.26. (a) and by Eq.37(b).

To calculate accurately the THDv, it is usually necessary to calculate all the significant side-band harmonics up to the fifth harmonic of the carrier. The frequency carrier depends on the number of pulses Ap (or the frequency modulation ratio m_f used). Calculating until the 899th harmonic and until Ap=79 (f_s=7.9Khz) as calculated from Eq.37 the THD vs. Ap is shown in Fig.5b. The dc link voltage Udc is chosen as the Ugrid (311.127 V). The minimum THDv is achieved for Ap=77 which is 48.88%. Has to be remembered that on the conventional unipolar SPWM each phase leg is switching at a frequency derived from the carrier signal frequency f_s. Since only one phase leg is modulated the carrier ratio for discontinuous modulation has to be double to all examples to achieve the same number of switch transitions for each phase leg over a complete fundamental cycle to compare it with the natural or regular sampled pwm schemes. So, for example if someone would like to compare the results of case A_p=21 (i.e. f_s=2.1kHz and f_p=1.05kHz), has to compare it with carrier frequency f_s=f_p=1.05kHz of a regular or natural sampled PWM in order to have the same switching transitions. The advantage of discontinuous PWM is that phase legs are stressed less than conventional PWM schemes.

6. Simulation and experimental results

To verify the proposed method, simulation and an experiment cases with two different numbers of pulses is implemented. In the first case Ap=11 is used, meaning a frequency modulation ratio of m_f =22 and switching frequency of the phase leg f_p=550Hz. In the second case Ap=21 is used meaning a frequency modulation ratio of m_f =42 and switching

frequency of each phase leg at f_p=1.05kHz. The simulation voltage output for both cases and its normalised FFT analysis are shown in Fig.6 and Fig.7, calculated for both cases until the 100th harmonic. The m_a =U_{max} /U_{pmm} ratio for both cases is the optimum-marginal. The proposed method is to be used for a grid tie VSI. Since for linear operation modulation ratio has to be kept below unity (m_a<1) the inverter never enters the over modulation region. As expected for unipolar discontinuous PWM the low order harmonics are clustered around multiples of m_f rather than $2m_f$ [17]. However, discontinuous switching halves the phase leg switching frequency for the same carrier frequency, since each phase leg is only modulated for 50% of the fundamental cycle. The dc link voltage Udc for simulation cases is chosen at 311.12 V for connection with the utility grid. For both cases U$_{1,rms}$ indicates the RMS voltage amplitude of the fundamental harmonic.
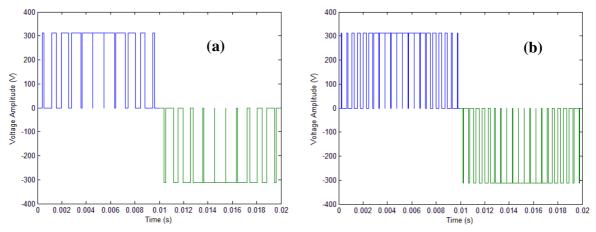

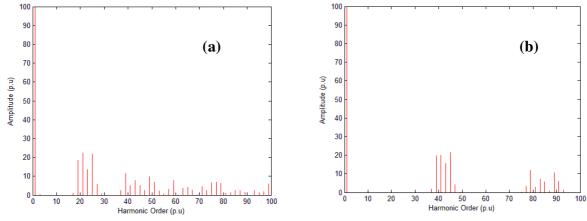Figure 6. Voltage Output for: (a) A$_p$=11 (f$_p$=550Hz) and (b) A$_p$=21 (f$_p$=1250Hz).

Figure 7. Voltage Spectrum for: (a) A$_p$=11 (f$_p$=550Hz, m$_a$=0.9966, THD=51.0845%, U$_{1,rms}$=219.4V) and (b) A$_p$=21 (f$_p$=1250Hz, m$_a$=0.99907, THD=48.4495%, U$_{1,rms}$=219.8V).

For experimental implementation a prototype inverter was constructed. The PWM scheme was implemented in MOSFETs IRF840 using an ATMEL ATMEGA328P. For better comparison, the number of pulses A$_p$ used were the same used in simulation. The voltage waveform and its frequency spectrum are shown in Fig.8 and Fig.9. It is obvious that the experimental results present very good correlation with simulation results.
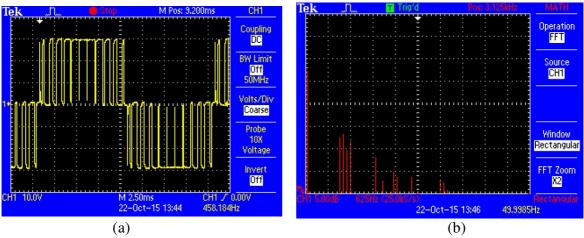
(a)   (b)

Figure 8. Experimental waveform with EAPWM (Ap=11). (a) Output voltage. (b) Frequency Spectrum.

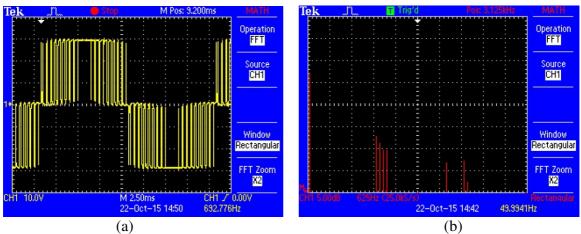(a)   (b)

Figure 9. Experimental waveform with EAPWM (Ap=21). (a) Output voltage. (b) Frequency Spectrum.

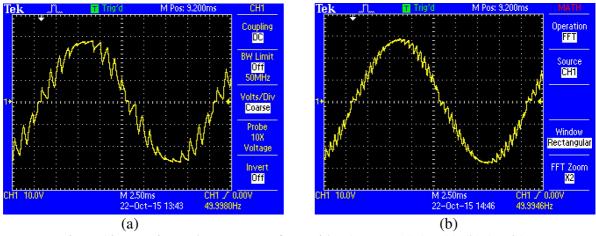(a)   (b)

Figure 10. Experimental current waveform with EAPWM. (a) Ap=11. (b) Ap=21.

In Fig.10 the current waveform is also presented for each case. The used inductor was L=25mH and the capacitor was C=2,2μF.

7. Conclusions and Further Work

The current study describes a contribution to the theory and first results for referential designed PWM waveforms. The described method based on well-defined equations, lets you set the desired amplitude modulation ratio between $0.1 < m_a < 1$. This algorithm has been modified to calculate the marginal m_a for a given switching frequency of the phase-leg (the number of pulses you set in the beginning). With this modification the m_a will be always close to one in order to meet the equal area criteria of the middle pulse. The significant advantage of the EAPWM is the well-defined mathematical formulation of the PWM that provides an ease of implementation in power systems, without the need of large computational effort. Further work will be carried out including the development of a new algorithm for the penetration in the overmodulation region introducing values of $m_a > 1$. Another aspect that will be taken in consideration for further work is the implementation of the Equal Areas theory in the field of the Multi-Level inverters where the direct EAPWM method will be applied for reference results.

References

[1] Holtz, J., "Pulsewidth modulation-a survey," Power Electronics Specialists Conference, 1992. PESC '92 Record., 23rd Annual IEEE , vol., no., pp.11,18 vol.1, 29 Jun-3 Jul 1992

[2] Holmes, D.; Lipo, T. Pulse Width Modulation for Power Converters: Principles and Practice Wiley-IEEE Press 2003 ISBN: 9780470546284

[3] Kim, Yoone Ho; Ehsani, M., "An Algebraic Algorithm for Microcomputer-Based (Direct) Inverter Pulsewidth Modulation," in Industry Applications, IEEE Transactions on , vol.IA-23, no.4, pp.654-660, July 1987

[4] Boglietti, A.; Griva, G.; Pastorelli, M.; Profumo, F.; Adam, T., "Different PWM modulation techniques indexes performance evaluation," Industrial Electronics, 1993. Conference Proceedings, ISIE'93 - Budapest., IEEE International Symposium on , vol., no., pp.193,199, 1993

[5] Rus, D. C.; Preda, N. S.; Incze, I.I.; Imecs, M.; Szabó, C., "Comparative analysis of PWM techniques: Simulation and DSP implementation," Automation Quality and Testing Robotics (AQTR), 2010 IEEE International Conference on , vol.3, no., pp.1,6, 28-30 May 2010

[6] Boost, M.A.; Ziogas, P.D., "State-of-the-art carrier PWM techniques: a critical evaluation," Industry applications, IEEE Transactions on , vol.24, no.2, pp.271,280, Mar/Apr 1988

[7] Patel, Hasmukh S.; Hoft, R.G., "Generalized Techniques of Harmonic Elimination and Voltage Control in Thyristor Inverters: Part I--Harmonic Elimination," Industry Applications, IEEE Transactions on , vol.IA-9, no.3, pp.310,317, May 1973

[8] Patel, Hasmukh S.; Hoft, R.G., "Generalized Techniques of Harmonic Elimination and Voltage Control in Thyristor Inverters: Part II --- Voltage Control Techniques," Industry Applications, IEEE Transactions on , vol.IA-10, no.5, pp.666,673, Sept. 1974, doi: 10.1109/TIA.1974.349239

[9] Zhiqiang Gao; Yunzhi Qiu; Xuesong Zhou; Youjie Ma, "An overview on harmonic elimination," in Mechatronics and Automation (ICMA), 2015 IEEE International Conference on , vol., no., pp.11-16, 2-5 Aug. 2015

[10] Trzynadlowski, A.M.; Gang, C., "Computation of optimal switching patterns for voltage-controlled inverters using neural-network software," Computers in Power Electronics, 1992., IEEE Workshop on , vol., no., pp.229,237, 1992

[11] Tengfei Wang; Yongqiang Zhu, "Analysis and comparison of multicarrier PWM schemes applied in H-bridge cascaded multi-level inverters," Industrial Electronics and Applications (ICIEA), 2010 the 5th IEEE Conference on , no., p.1379,1383, 15-17 June 2010

[12] Konstantinou, G.S.; Pulikanti, S.R.; Agelidis, V.G., "Harmonic elimination control of a five-level DC-AC cascaded H-bridge hybrid inverter," Power Electronics for Distributed Generation Systems (PEDG), 2010 2nd IEEE International Symposium on , vol., no., pp.352,357, 16-18 June 2010

[13] Zhang Wenyi; Meng Xiaodan; Li Zhenhua, "The simulation research for selective harmonic elimination technique based on genetic algorithm," in Control Conference (CCC), 2014 33rd Chinese , vol., no., pp.8628-8632, 28-30 July 2014

[14] Yang Ke-hu; Yuan Zhi-bao; Wei Wei; Yuan Ru-yi; Yu Wen-sheng, "Solve the selective harmonic elimination problem with groebner bases theory," in Control Conference (CCC), 2015 34th Chinese , vol., no., pp.7910-7915, 28-30 July 2015

[15] D. Nafpaktitis,G. Hloupis,I. Stavrakas,F. Paterakis., "An Alternative Approach for PWM Modeling in Power Electronics Systems", J. Electrical Systems 7-4 (2011): 438-447

[16] Bowes, S.R., "Comments, with reply, on "An algebraic algorithm for microcomputer-based (direct) inverter pulsewidth modulation" by Y.H. Kim and M. Ehsani," in Industry Applications, IEEE Transactions on , vol.24, no.6, pp.998-1004, Nov.-Dec. 1988

[17] Mohan, N, Undelend, T., Robbins, W, "Power electronics converters – Application and design", J.Wiley and sons, USA, 1995.

[18] D.Grahame Holmes, Thomas A. Lipo, "Pulse Width Modulation for Power Converters-Principles and Practice", IEEE series on Power Engineering, J.Wiley and sons, USA, 2003.